Article

Chinese Science Bulletin

Engineering Thermophysics

May 2011 Vol.56 No.15: 1603–1610
doi: 10.1007/s11434-010-4188-y

Boundary velocity slip of pressure driven liquid flow in a micron pipe

ZHOU JianFeng*, GU BoQin & SHAO ChunLei

College of Mechanical and Power Engineering, Nanjing University of Technology, Nanjing 210009, China

Received May 21, 2010; accepted August 11, 2010; published online April 13, 2011

The velocity slip of gas flow in a micron channel has been widely recognized. For pressure driven liquid flow in a macro pipe, the minute velocity slip at the wall boundary is usually neglected. With a decreasing scale in the cross section of the flow passage, the effect of velocity slip on flow and heat transfer behaviors becomes progressively more noticeable. Based on the three Hamaker homogeneous material hypotheses, the method for calculating the acting force between the solid and liquid molecular groups is established. By analyzing the forces exerted on the liquid group near the pipe wall, it is found that the active force arising from the rough solid wall can provide the component force to resist the shearing force and keep the liquid group immobile. Based on this a velocity slip criterion is proposed. Considering the force balance of a slipping liquid group, the frictional force caused by the solid wall can be obtained and then the velocity of the liquid group can be calculated using the derived coefficient of friction. The investigation reveals that, in a micron pipe, a small velocity slip may occur when the flow pressure gradient is relatively large, and will cause errors in the pipe flow estimates.

velocity slip, pressure driven, liquid molecular group, coefficient of friction

Citation: Zhou J F, Gu B Q, Shao C L. Boundary velocity slip of pressure driven liquid flow in a micron pipe. Chinese Sci Bull, 2011, 56: 1603–1610, doi: 10.1007/ s11434-010-4188-y

Fluid flows in the channels of micro pumps, valves, ejectors and mixers are usually driven by pressure differences. These micro channels with diameters ranging from nanometers to microns are the functional elements of heat and mass transmission in microfluidic systems. The effects of the surface topography and acting force of the solid boundary wall will result in the deviation of the flow behavior of the fluids at microvolumes from the flow in macro channels. Consequently, increasing attention is being paid to the velocity slip at the wall boundary.

The velocity slip has a great influence on the velocity and temperature distributions of fluid flow. The basic assumption in classical fluid dynamics is that the velocity of fluid at the wall boundary is strictly in accordance with that of a wall. However, research has revealed that once the shear rate is larger than a critical value, there will be velocity discontinuities and slip near the wall boundary. Most investigations on velocity slip concentrate on gas flow in micron channels because of the relatively small viscosity and large spacing voids between gas molecules. Based on the Maxwell first-order velocity-slip boundary condition, Xie et al. [1] introduced the second-order velocity-slip boundary conditions into the Navier-Stocks Equations to expand their field of application. Sparrow et al. [2] found that both the drag coefficient and the coefficient of heat transfer in micro circular pipes are smaller than in macro scale pipes. The velocity slip and temperature jump are considered in analyzing the Graetz problem [3], and the two conditions are also used in solving the Navier-Stokes and energy equations for the incompressible gas flow in micro annular channels [4] and rectangular channels [5]. Xu et al. [6] found that the velocity slip is largely determined by the fluid temperature and attractive force of the wall.

Because of the complication and difficulty of measuring

*Corresponding author (email: zhoujianfeng@njut.edu.cn)

in the very small scale of the micron gap, the value of velocity slip is very difficult to measure directly. The molecular dynamic simulation method has been widely applied in the study on velocity slip of gas flow in nano channels. Thompson investigated the velocity slip of liquid argon film using the spherical molecular model [7]. Wang et al. performed a molecular dynamics study of the interfacial slip behavior of ultrathin lubricating films [8]. The non-equilibrium molecular dynamics simulation was used by Cao et al. [9] to investigate the Couette flow in nanochannels, and different slip behaviors, such as velocity slip, interfacial no-slip and negative slip, were found. The velocity slip in a nanometer fluid film, which increases rapidly with increasing film thickness, was found to occur for relatively small shear rates [10]. Later research indicates that the lamination and slip between adjacent layers always exist in a nanometer lubrication film [11]. Bao et al. investigated the flow and heat transfer in micro Couette and Poiseuille flow using the Burnett simulation method [12–14]. Wu et al. studied the pressure driven transient flow of an incompressible Newtonian fluid in micro tubes with a Navier slip boundary condition [15]. Furthermore, the velocity slip of the lubrication film was experimentally investigated by Yuan et al. [16], Miao et al. [17], Zhou et al. [18] and Wu et al. [19], including its existence in sliding bearings. However, when the cross-section of the pipe is of micron scale, the molecular dynamics simulation method becomes inappropriate because of the very large number of molecules.

Considering that the viscosity of liquid is usually larger than that of gas, the velocity slip of liquids in micro channels and pipes is often neglected when analyzing the flow characteristics. However, in a high precision flow instrument with nanometer or micron pipes, the velocity slip will influence the flow to some extent. This paper presents a theoretical analysis of the velocity slip of liquid flow in micron pipes. The velocity slip criterion will be put forward to identify whether the slip of the liquid layer near wall boundary will occur or not, and the method for calculating the value of velocity slip will also be given.

1 Model of pressure driven liquid flow in micro circular pipe

Figure 1 illustrates the lengthwise section of a circular pipe, where p_1 and p_2 are the inlet and outlet pressures; r and z are the radial and axial coordinates; $v(r)$ is the velocity distribution function of liquid and Δv is the value velocity slip.

Compared with the inner radius, the degree of roughness of the inner wall cannot be neglected and the flow is assumed to be a laminar current of Newtonian fluid. According to the Newtonian shear law, $v(r)$ is of the form

$$v(r) = -\frac{\Delta p}{L}\frac{r^2}{4\mu} + \frac{C_1}{\mu}\ln r + C_2, \tag{1}$$

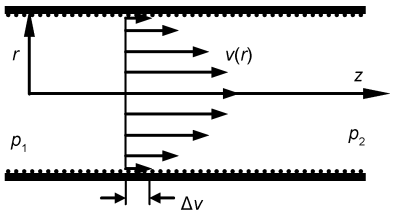

Figure 1 Model of pressure driven flow in circular pipe.

where $\Delta p=p_1-p_2$, μ is the dynamic viscosity of fluid and L is the length of the pipe. C_1 and C_2 are undetermined constants that can be solved using the two boundary conditions, namely the zero shearing stress at $r=0$ and the velocity at the wall boundary $v(R)=\Delta v$. Hence $v(r)$ can be expressed by

$$v(r) = \frac{\Delta p}{4\mu L}\left(-r^2 + R^2\right) + \Delta v, \tag{2}$$

where R is the inner radius of the pipe. The shearing force distribution along r can be expressed by

$$\tau(r) = -\frac{\Delta p}{2L}r. \tag{3}$$

Eq. (3) indicates that the shearing stress is relative to the pressure gradient along axis z and the radius r. The velocity slip Δv does not affect the distribution of shearing stress $\tau(r)$.

2 Calculation of acting force between solid wall and liquid

The viscosity of liquid, which is initiated by cohesion and adhesion forces between molecules, makes it possible to adhere to the solid wall, and it appears only when the liquid is bearing a shearing stress. However, the acting forces between liquid molecules always exist because of their potential energy. Because the movements of liquid molecules are highly random, it is impossible to calculate the total acting force between a solid wall and fluid by counting all the acting forces arising from innumerable solid and fluid molecular pairs.

2.1 Acting force between molecular groups

The three Hamaker hypotheses give the theoretical basis to resolve a discrete problem by the integration method, which can be described by (1) The force between two substances is the sum of the forces on molecular pairs (each of the molecules in M_1 generates pairs with every molecule in M_2, in Figure 2). (2) The substance is made up infinitesimally by the volume dv and the digital density ρ continuously. (3) For one substance, the digital density ρ and the constants of repulsive and attractive forces are invariant. The three hypotheses have

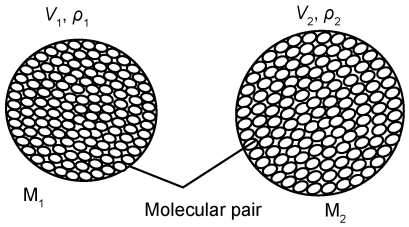

Figure 2 Model of fluid molecular groups.

been well developed [20, 21] and applied. According to the three Hamaker homogeneous material hypotheses, the continuous liquid can be assumed to be made up of numbers of fluid molecular groups with certain shapes and digital densities. Each group is composed of homogeneous molecules. Figure 2 shows the models of fluid molecular groups M_1 and M_2, where V_1 and V_2 are the contained volumes of the boundaries of M_1 and M_2. The two groups are composed of many discrete fluid molecules and these molecules are assumed to be stationary. Then the calculation of the acting forces between randomly moving molecules can be substituted by calculating the acting force between the two molecular groups consisting of stationary molecules.

The Lennard-Jones 12-6 potential model is used to calculate the force of any molecular pair, which can be expressed by

$$U = 4\varepsilon\left[\left(\frac{\sigma}{l}\right)^{12} - \left(\frac{\sigma}{l}\right)^{6}\right]. \tag{4}$$

The inner forces between the molecules in a group have no influence on the motion of the group, therefore only the force between one molecule in M_1 and the other molecule in M_2 is considered. The molecular force initiated by the Lennard-Jones potential can be calculated by

$$f(l) = \frac{A}{l^{13}} - \frac{B}{l^{7}} = f_1(l) - f_2(l), \tag{5}$$

where $f_1(l)$ is the repulsive force and $f_2(l)$ is the attractive force, and A and B are constants. The total acting force between M_1 and M_2 can be obtained by integrating $f(l)$:

$$F = \rho_1\rho_2 \iint_{V_2V_1} \left[f_1(l) - f_2(l)\right] \mathrm{d}v_1 \mathrm{d}v_2, \tag{6}$$

where ρ_1 and ρ_2 are the digital densities of M_1 and M_2.

So far, only the complicated analytical equation for calculating the acting force between two groups with spherical boundaries has been derived [20–22]. For the rectangular group used in this paper, the integration procedure is too complex to give the corresponding analytical equations. Hence, the acting force is calculated by a numerical integration method.

2.2 Geometrical parameters of molecular group

Although the molecular group size is larger than the diameter of a molecule, it is much smaller than the radius and length of a micron pipe. Considering the liquid layer near the solid wall, a rectangular group with width w_1 can be extracted from the layer and the corresponding wall group with width w_2 is also established, as Figure 3 illustrates. h_1 and h_2 are the heights of the two groups, and Δ is the clearance between the two groups. These geometrical parameters should be determined according to the effective range of the acting force. The thickness of the two groups is 1×10^{-8} m.

The fluid in the analysis is liquid argon (Ar), the solid molecule is an assumptive one (X), and their potential energy equations are both in the form of eq. (4). The physical parameters of molecules Ar and X are listed in Table 1.

The collision diameter of liquid and solid molecules σ_{12} can be calculated by

$$\sigma_{12} = \sigma_1 \frac{d_1 + d_2}{2d_1}. \tag{7}$$

Because the two groups are symmetrical about the coordinate y, the acting force component along coordinate x is zero. The effect of clearance δ on the acting force is very obvious, as can be seen in Figure 4, where F_y is the force component along coordinate y. In the range of δ from 1×10^{-14} to 1×10^{-12} m, the change in F_y is small because of the interaction between attractive and repulsive forces. Once δ is larger than 1×10^{-12} m, F_y reduces rapidly. In this example, h_1=h_2=1×10^{-8} m, w_1=w_2=1×10^{-8} m. The attractive force is much larger than the repulsive force. Therefore, the resultant force makes the two groups attract each other. The appropriate value of δ is 1×10^{-13} m.

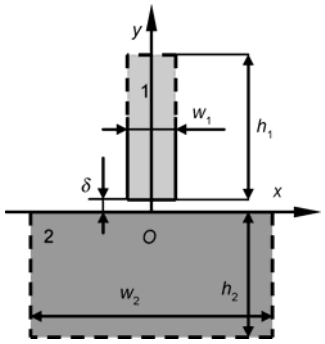

Figure 3 Rectangular models of liquid and solid groups. 1, Liquid molecular group; 2, solid molecular group.

Table 1 Physical parameters of molecules

	Variable subscript	Molecular quality m (kg)	Potential energy constant ε (J K^{-1})
Ar	1	6.633×10^{-26}	1.67×10^{-21}
X	2	–	8.35×10^{-21}
	Collision diameter σ (m)	Spacing interval d (m)	Digital density ρ (m^{-3})
Ar	3.47×10^{-10}	3.71×10^{-10}	1.94×10^{28}
X	2.75×10^{-10}	2.17×10^{-11}	7.80×10^{28}

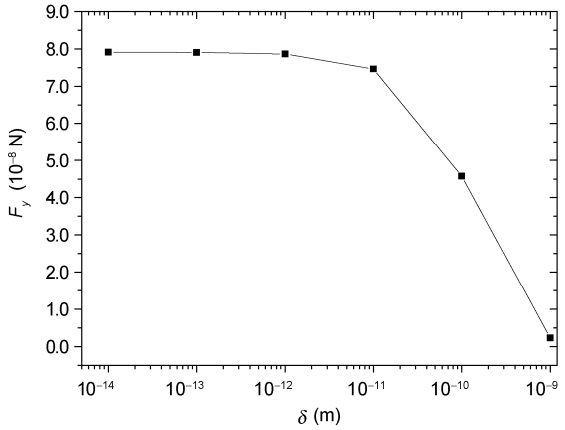

Figure 4 Change of F_y with δ.

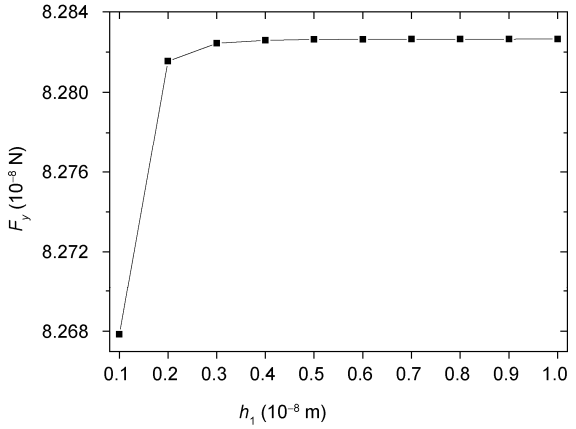

Figure 6 Change of F_y with h_1.

The change regularity of F_y with w_1 can be seen in Figure 5, here h_1=1×10^{-8} m, w_2=1×10^{-8} m, h_2=1×10^{-8} and δ=1×10^{-13} m. F_y increase when w_1 increases from 1×10^{-8} to 2×10^{-8} m, but it barely changes when w_1>2×10^{-8} m.

Similarly, when w_1=1×10^{-8} m and w_2 increases from 1×10^{-8} to 1×10^{-7} m, the range of w_2 which results in the increase of F_y is also from 1×10^{-8} to 2×10^{-8} m. Therefore, for the given liquid molecular group, the effective width of the solid group is suggested to be double the width of the liquid group.

Figure 6 illustrates the change regularity of F_y with the increasing h_1. Because the acting range of potential molecular energy is only several times as great as the collision diameter σ, once h_1>4×10^{-9} m, the increase of h_1 will not result in an obvious increase of F_y. The increase of h_2 results in a similar regularity to that shown in Figure 6. Therefore, h_1=1×10^{-8} m and h_2=1×10^{-8} m can satisfy the calculation precision of the maximum acting force between the two groups.

The acting force between two liquid molecular groups (Figure 7) is a little smaller than that between the liquid and solid groups because the potential energy of solid molecules is larger than that of liquid molecules, as can be seen in Figure 8, where w_1=1×10^{-8} m and δ=1×10^{-13} m. Figure 8 indicates that the acting force between the two liquid molecular groups is also limited. Hence, it is possible for the solid wall to attract the liquid group because the attractive force arising from the solid wall may be larger than that from the above liquid group.

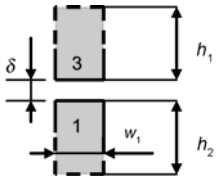

Figure 7 Model of two liquid molecular groups. 1, Liquid molecular group; 3, above liquid molecular group.

3 Occurrence of boundary velocity slip

3.1 Shearing stress in liquid layers near a solid wall

There are two adjacent liquid groups in Figure 9. When affected by shearing stress and velocity gradients, the two groups *a-b-c-d* and *e-f-g-h* will deform to be *a′-b′-c′-d′* and *e′-f′-g′-h′* respectively after a time step. In this process, the component forces F_x and F_y between the two groups will

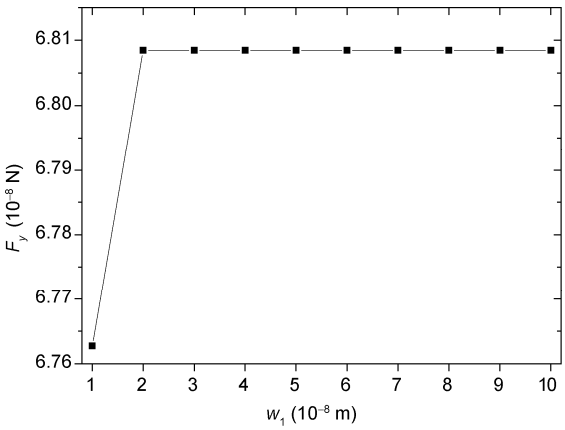

Figure 5 Change of F_y with w_1.

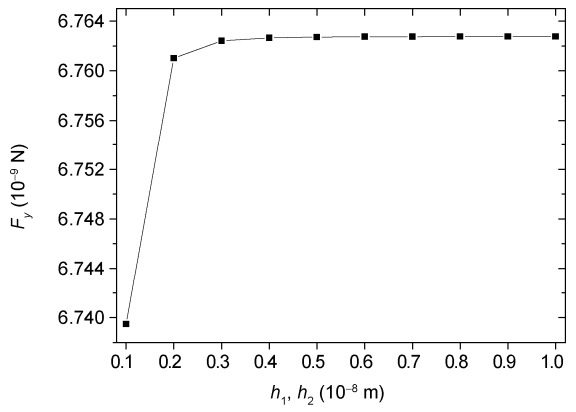

Figure 8 Change of F_y with h_1 and h_2.

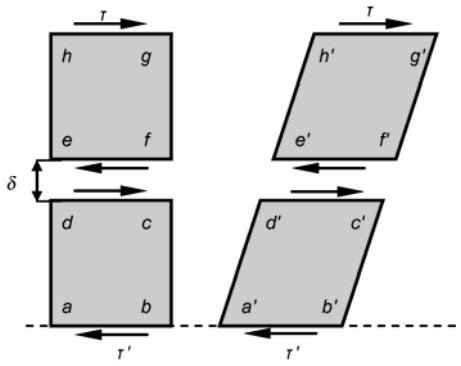

Figure 9 Shear model of two adjacent liquid groups.

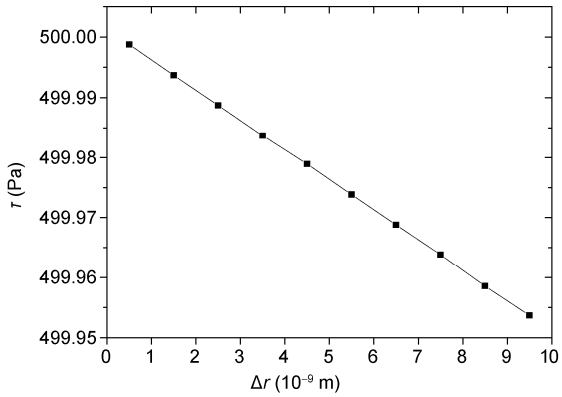

Figure 11 Shearing stress τ vs. Δr.

change with the angular deformation α, as Figure 10 illustrates.

When the two groups are moving relative to each other, the component forces F_x and F_y are not constant and do not relate to the velocity. The component force F_x cannot be regarded as the shearing force between the two groups because the shearing force must be relative to the velocity gradient. Therefore, the shearing force between the two groups cannot be calculated using the method proposed in Section 2.1.

According to eq. (3), the shearing stress in liquid layers near a solid wall can be calculated, and the result is shown in Figure 11. The calculating parameters are: R=1.0×10^{-3} m, L=0.1 m, p_1=1.1×10^5 Pa, p_2=1.0×10^5 Pa and Δr=R–r. It is obvious that the shearing stress τ changes linearly along the radial direction and the maximum shearing stress is located at the wall boundary.

3.2 Forces on liquid group near solid wall

The real surface of the solid wall is rough, with randomly distributed peaks and valleys. At nanometer dimensions, the surface is composed of solid molecules, which are always exposed to liquid molecules. The direction of the acting force exerted on the liquid group can be along the direction ***n*** shown in Figure 12(a), or it can be along ***n′*** shown in Figure 12(b) on the premise that θ is relatively small.

If the direction of the acting force exerted on the liquid molecular group is normal to the direction of shearing stress arising from the above liquid group 3, the liquid molecular group 2 cannot remain stationary. Under the effect of the shearing force, the liquid group 2 will deflect and the direction of the acting force will also change. The component of the acting force may then resist the shearing force and the liquid group may be stationary.

The simplified rough surface of the solid wall is composed of inclined surfaces, as Figure 13 illustrates. The inclination angle η relates to the inclination degree of the liquid group, and the change of roughness of the solid wall can be realized by changing the dimension l when η is given.

The forces exerted on the liquid molecular group can be seen in Figure 14. F_y is the acting force arising from the solid group, F_s is the shearing force and the F_u is the acting force arising from the above liquid group. If the sum of the three forces equals zero, the group can be stationary.

The area of the upper surface of the liquid group is constant in the following analysis. Because of the deformation of the group, both F_y and F_u will change during the course of deformation. With the increase of F_s, θ decreases correspondingly,

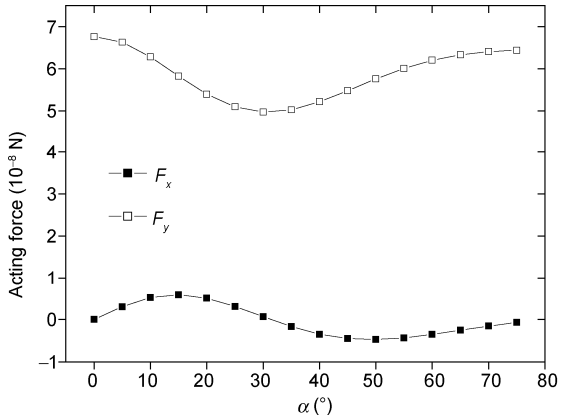

Figure 10 Changes of F_x and F_y with angular deformation α.

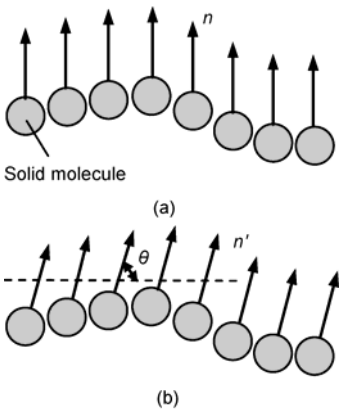

Figure 12 Direction of acting force arising from solid.

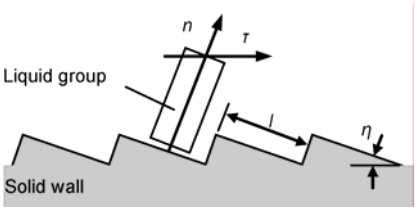

Figure 13 Rough solid wall and near liquid molecular group.

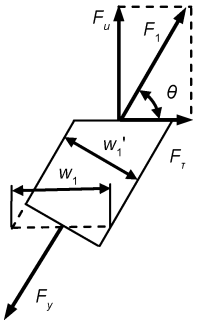

Figure 14 Forces on liquid group near rough wall.

and the change of the resultant force F_1 is unknown. For the solid surface, the width of the liquid group changes from w_1 to w_1', and $w_1' = w_1 \sin\theta$. Because F_u is a complicated function of θ and θ=arctan(F_u/F_s), θ is solved according to the flow process shown in Figure 15.

3.3 Slip of liquid molecular group

The operation condition which influences the shearing stress at the wall boundary is the pressure gradient $\Delta p/L$. The change regularities of F_1 and F_y with the increase in pressure gradient are illustrated in Figure 16, where k=Δp/2L.

Both F_1 and F_y reduce when k increases, but the decreasing amplitude of F_y is generally smaller than F_1. When k>8.7×10^3 Pa m^{-1}, F_y is smaller than F_1, which means the solid group cannot drag the liquid group any more, and slip of the liquid group occurs.

Except for the operation parameters, the parameters in

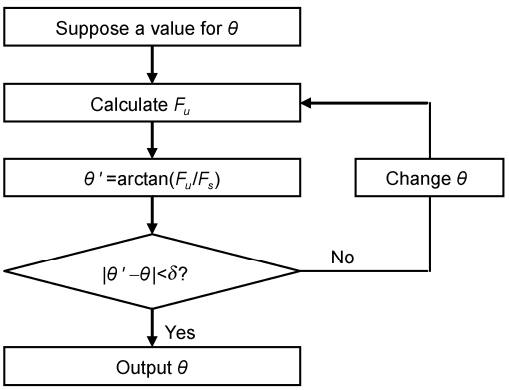

Figure 15 Flow process of calculating θ.

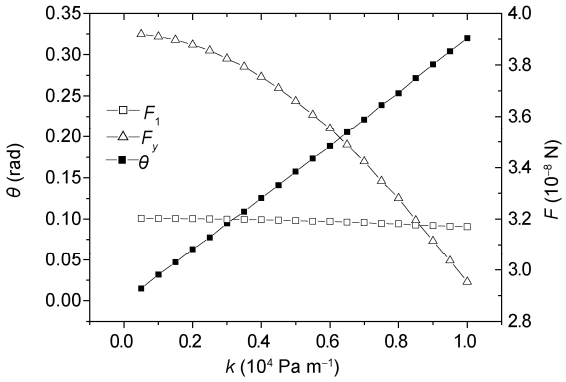

Figure 16 Changes of F_1 and F_y with k.

the potential energy equation of the molecules also contribute to the slip velocity of the liquid group. For instance, if the potential energy constant of liquid molecules ε_1 increases, the difference between ε_1 and ε_2 reduces and the value of k results in the slip of liquid group being less than 8.7×10^3 Pa m^{-1}.

4 Calculation of slip velocity

4.1 Forces on slipping liquid group

Once the slip of the liquid group occurs, the direction of the force F_y exerted on the liquid group is normal to the wall. Moreover, the frictional force arising from the rough wall F_f will be exerted on the liquid group (Figure 17). F_{p1} and F_{p2} are generated by liquid pressure on the left and right sides of the liquid group.

These forces shown in Figure 16 should satisfy the equilibrium conditions expressed by

$$F_u = F_d, \tag{8}$$

$$F_{p1} - F_{p2} + F_\tau = F_f. \tag{9}$$

4.2 Coefficient of friction of liquid at wall boundary

The movement of a molecule is always inhibited by the acting forces arising from the surrounding molecules, and this retarding effect can be defined as the frictional force. The frictional force linearly relates to the velocity of the molecule [23], and can be expresses by

$$F(t) = -\beta m v + G(t), \tag{10}$$

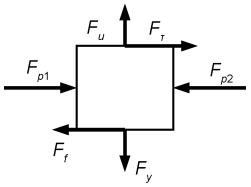

Figure 17 Forces on liquid group under slip conditions.

where $G(t)$ is the randomly undulant force, β is the coefficient of friction, m and v are the quality and velocity of the molecular.

Rice et al. [24] gave the expression of β in spherical coordinates:

$$\beta=\left[\frac{\rho}{3m}\int_0^{2\pi}\int_0^{\pi}\int_0^{\infty}r^2\left(\frac{\partial^2U}{\partial r^2}+\frac{2}{r}\frac{\partial U}{\partial r}\right)g(r)\sin\theta\mathrm{d}r\mathrm{d}\theta\mathrm{d}\phi\right]^{1/2}, \quad (11)$$

where ρ is the number density of the molecular liquid, and $g(r)$ is the equilibrium radial distribution function of the molecules, which holds

$$g(r)=\exp\left[-\frac{U}{k_bT}\right], \quad (12)$$

where T is absolute temperature and k_b is the Boltzmann constant.

Generally, the solid molecules will influence the distribution of the near liquid molecules, so two assumptions are put forward to counter the effect of solid molecules: (1) The distribution of liquid molecules cannot be changed by solid molecules and the acting forces between liquid molecules cannot be disturbed by solid molecules; (2) The solid molecules distribute homogeneously and the equilibrium radial function is equal to 1.

Figure 18 illustrates a spherical volume; the liquid molecule whose coefficient of friction β is to be determined is located at the wall boundary where the center of the spherical volume is located. The retarding effect on the liquid molecules arises from the solid and liquid molecules in the volume.

For the upper half of the sphere v_1, the coefficient β_1 can be calculated using

$$\beta_1=\left[\frac{\rho}{3m}\int_0^{2\pi}\int_0^{\pi/2}\int_0^{\infty}r^2\left(\frac{\partial^2U}{\partial r^2}+\frac{2}{r}\frac{\partial U}{\partial r}\right)g(r)\sin\theta\mathrm{d}r\mathrm{d}\theta\mathrm{d}\phi\right]^{1/2}. \quad (13)$$

The coefficient β_2 for the lower half of the sphere v_2 can be obtained from [25]

$$\beta_2=\left[\frac{1}{3m}(f_2-f_1)\right]^{1/2}, \quad (14)$$

where

$$f_1=\rho\int_0^{2\pi}\int_0^{\pi/2}\int_0^{\infty}r^2\left(\frac{\partial^2U}{\partial r^2}+\frac{2}{r}\frac{\partial U}{\partial r}\right)g(r)\sin\theta\mathrm{d}r\mathrm{d}\theta\mathrm{d}\phi, \quad (15)$$

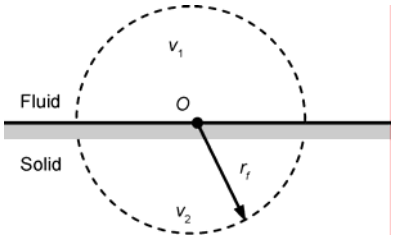

Figure 18 Spherical volume for calculating coefficient of friction.

$$f_2=\rho_s\int_0^{2\pi}\int_0^{\pi/2}\int_0^{\infty}r^2\left(\frac{\partial^2U_s}{\partial r^2}+\frac{2}{r}\frac{\partial U_s}{\partial r}\right)\sin\theta\mathrm{d}r\mathrm{d}\theta\mathrm{d}\phi, \quad (16)$$

where ρ_s and U_s are the number density and potential energy function of the solid molecules. Then the coefficient of friction of the liquid molecules β can be obtained by

$$\beta=\sqrt{\beta_1^2+\beta_2^2}. \quad (17)$$

Eqs. (13), (15) and (16) can be solved by numerical integration methods. With the parameters listed in Table 1, the coefficient of friction of the liquid at the wall boundary is 1.961×10^{13} s^{-1}. Using this coefficient and eq. (9), the slip velocity Δv, namely the velocity of the liquid molecular group near the solid wall, is obtained and increases with the increasing pressure difference Δp, as Figure 19 illustrates.

Although the magnitude of the velocity slip Δv is small, the velocity slip does exist in the pressure driven micron pipe. The flow error induced by Δv will become more and more obvious when the radius of the pipe reduces. For example, when Δp= 0.5×10^5 Pa and R= 6.25×10^{-5} m, the flow error initiated by Δv is about 0.37%. If the inner radius of the pipe decreases, the error will be enlarged.

The velocity slip exhibits the proportional relationship with the pressure difference, and that is in accordance with the experimental results given in [16] and [17]. So for there is no analytic equation for calculating the velocity slip of fluid flow in a pipe, and the theoretical results should be verified by experiments. To describe the slip characteristics of fluid on the solid surface, Navier introduced a general boundary condition, namely the fluid velocity component tangential to the solid surface and relative to the solid surface, which is proportional to the shear stress on the fluid–solid interface, as expressed by

$$\Delta v=-l^*\frac{\tau(R)}{\mu}, \quad (18)$$

where l^* is the slip length which can be determined according to eq. (19) by measuring the flow rate Q [15].

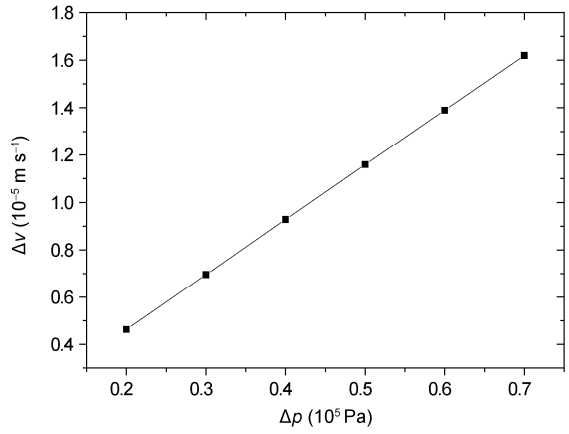

Figure 19 Velocity slip Δv vs. pressure difference Δp.

$$\frac{2\mu L}{\pi R^3 \Delta p} Q = l^* + \frac{R}{4}. \tag{19}$$

If l^*=0, there is no velocity slip occurring. Once l^*>0, this indicates that velocity slip at the wall boundary exists, and the real flow rate must be larger than that corresponding to the zero velocity slip condition. Future research will aim at revealing the velocity slip regularity of fluid flow in a micron pipe by an experimental method.

Using the Hamaker hypotheses, the randomness of fluid molecular movement is ignored; therefore, the effect of temperature on the slip velocity cannot be considered. Furthermore, according to the kinetic theory, the slip velocity is mainly determined by the collision process among the fluid molecules and the solid wall which can be characterized by direct reflection and scattered reflection. The effect of the surface topography of the solid wall is not considered, either.

5 Conclusions

The liquid velocity slip at the wall boundary of a micron pipe, which has great influence on the flow and heat transfer behaviors, is investigated. The velocity slip is mainly related to the wall property and shearing stress of the liquid at the wall boundary.

This paper provides a method to determine the velocity slip condition based on the force analysis for the liquid group near the solid wall. The mass distribution of the liquid molecules is considered to be continuous and the acting force between the liquid and solid wall can be calculated by an integration method without considering the random motion of molecules. The appropriate geometrical parameters of the liquid molecular group are determined by analyzing the effective action range of the molecular force. The simplified rough surface can drag the liquid group on the basis that the acting force arising from solid wall can provide enough component force to resist the shearing force. The potential energy parameters of liquid and solid molecules and the shearing stress in the liquid influence the condition of velocity slip occurring.

Once the velocity slip of the liquid group occurs, the liquid group will bear the frictional force induced by the solid wall. The frictional force is directly proportional to the velocity of the liquid group. Using the derived coefficient of friction of liquid molecules, the magnitude of the velocity slip can be obtained.

This work was supported by the National Natural Science Foundation of China (10872088), the Doctoral Foundation of Ministry of Education of China (20070291004 and 20093221120009) and the Academic Discipline Construction Fund of Nanjing University of Technology.

1 Xie C, Fan J. Assessment of second-order velocity-slip boundary conditions of the Navier-Stocks equations (in Chinese). Chin J Theor Appl Mech, 2007, 39: 1–6
2 Sparrow E M, Lin S H. Laminar heat transfer in tubes under slip-flow conditions. ASME J Heat Transfer, 1962, 84: 363–369
3 Barron R F, Wang X M, Ameel T A, et al. The Graetz problem extended to slip-flow. Int J Heat Mass Transfer, 1997, 40: 1817–1823
4 Zhu X, Xin M D. Laminar Flow and heat transfer in micro-annular channel in slip flow regime (in Chinese). J Eng Thermophys, 2001, 22: 203–206
5 Xiao R, Xin M D, Zhu X. Analysis of gaseous slip flow and heat transfer in micro rectangular channels (in Chinese). J Chongqing Univ (Nat Sci Ed), 2004, 24: 99–103
6 Xu C, He Y L, Wang Y. Molecular dynamics studies of velocity slip phenomena in a nanochannel (in Chinese). J Eng Thermophys, 2005, 26: 912–914
7 Thompson P A, Robbins M O. Shear flow near solids: Epitaxial order and flow boundary conditions. Phys Rev A, 1990, 41: 6830–6837
8 Wang H, Hu Y Z, Guo Y. Molecular dynamics study of in terfacial slip behavior of ultrath in lubricating films (in Chinese). J Tsinghua Univ, 2000, 40: 107–110
9 Cao B Y, Chen M, Guo Z Y. Molecular dynamics studies of slip flow in nanochannel (in Chinese). J Eng Thermophys, 2003, 24: 670–672
10 Wang H, Hu Y Z, Zou K, et al. Nano-tribology through molecular dynamics simulations (in Chinese). Sci China Ser A, 2001, 44: 1049–1055
11 Zeng F L, Sun Y. Molecular dynamics simulation of nano-scale thin film lubrication and its modification (in Chinese). Chin J Mech Eng, 2006, 42: 138–143
12 Bao F B, Lin J Z, Shi X. Burnett simulations of flow and heat transfer in micro couette flow using second-order slip conditions. Heat Mass Transfer, 2007, 43: 559–566
13 Bao F B, Lin J Z. Burnett simulation of gas flow and heat transfer in micro Poiseuille flow. Int J Heat Mass Transfer, 2008, 51: 4139–4144
14 Bao F B, Lin J Z. Burnett simulations of gas flow in microchannels, Fluid Dyn Res, 2008, 40: 679–694
15 Wu Y H, Wiwatanapataphee B, Hu M B. Pressure-driven transient flows of Newtonian fluids through microtubes with slip boundary. Physica A, 2008, 387: 5979–5990
16 Yuan B, Zhang G X, Wu B Y, et al. Study on the interface slippage of EMP circular sliding bearing (in Chinese). Lubr Eng, 2001, 2: 29–30, 42
17 Miao X X, Wang Q F, Chen X C, et al. Experiment and study on wall slip of lubricating grease flowing in tube (in Chinese). J Harbin Inst Technol, 2007, 39: 1172–1176
18 Zhou H W, Zhang Y H, Li A M, et al. Experimental study on moving boundaries of fluid flow in porous media. Chinese Sci Bull, 2008, 53: 2438–2445
19 Wu C W, Ma G J. On the boundary slip of fluid flow. Sci China Ser G: Phys Mech Astron, 2005, 48: 178–187
20 Tian W C, Jia J Y. Definition domain analyzing of micro continuous medium method (in Chinese). Chin J Comput Mech, 2005, 22: 189–192
21 Tian W C, Jia J Y. Amelioration of the hamaker homogeneous material hypothesis (in Chinese). Chin Phys Soc, 2003, 52: 1061–1065
22 Dedkov G V, Dyshekov M B. Deformation of the contact region and adhesional friction between nanoprobe and surface. Surf Sci, 2000, 463: 125–134
23 Kirkwood J G. The statistical mechanical theory of transport processes I: General theory. J Chem Phys, 1946, 14: 180–201
24 Rice S A, Kirkwood J G. On an approximate theory of transport in dense media. J Chem Phys, 1959, 31: 901–908
25 You X Y, Zheng X J, Li D. Theoretical study on friction coefficient of liquid in microchannels (in Chinese). China Mech Eng, 2005, 16: 1278–1281